American Mineralogist, Volume 91, pages 1197–1200, 2006

LETTER

Terrestrial analogs of martian sulfates: Major and minor element systematics of alunite–jarosite from Goldfield, Nevada

J.J. PAPIKE, J.M. KARNER,* M.N. SPILDE, AND C.K. SHEARER

Institute of Meteoritics, Department of Earth and Planetary Sciences, University of New Mexico, Albuquerque, New Mexico, 87131, U.S.A.

ABSTRACT

Alunite and jarosite from Goldfield, Nevada, show spectacular relationships between early alunite and later jarosite. In some cases, jarosite overgrows alunite with the same crystallographic orientation and sharp contacts. Electron microprobe analyses of these phases show that they fall in the alunite-jarosite quadrilateral defined by alunite, $KAl_3(SO_4)_2(OH)_6$; natroalunite, $NaAl_3(SO_4)_2(OH)_6$; jarosite, $KFe^{3+}_3(SO_4)_2(OH)_6$; and natrojarosite, $NaFe^{3+}_3(SO_4)_2(OH)_6$. A large compositional gap occurs between alunite-natroalunite and jarosite-natrojarosite. This gap has no crystal chemical basis because Al and Fe^{3+} can readily substitute for each other in octahedral site coordination. We believe the "on-off switch" behavior between early alunite and later jarosite is caused by an oxidant entering the system, oxidizing Fe^{2+} in solution to Fe^{3+}, raising the Eh and possibly oxidizing H_2S to lower the pH, and thus stabilizing jarosite relative to alunite. The activity of Fe (as Fe^{2+}) increased in the solution because of prolonged alunite crystallization but could not readily enter the crystal structure until it was oxidized to Fe^{3+}. The jarosite overgrowths show striking oscillatory zoning of Na- and K-rich bands. This reflects up to an order of magnitude change in the fluid K/Na ratio. These textures are interpreted to represent rapid growth and kinetic control of delivery of free Na and K to the crystal-fluid interface. This could be due to some combination of Na and K diffusion rates in the solution and complex ion breakdown involving Na and K.

Keywords: Jarosite, Mars, electron microprobe, terrestrial analogs

INTRODUCTION

Martian jarosite was identified using data collected by the Mars Exploration Rover (MER) Mössbauer instrument (Klingelhöfer et al. 2004). The Mössbauer instrument identified jarosite and hematite as important phases in outcrop and regolith of the equatorial site Meridiani Planum, but could not provide the detailed chemistry (major, minor, and trace), stable isotope data for S, H, and O, or ages from Ar–Ar or K–Ar techniques that terrestrial laboratories have provided for terrestrial samples. Martian jarosite could have formed from low-temperature processes (e.g., McLennan et al. 2005) or high-temperature (hydrothermal) processes (e.g., McCollom and Hynek 2005; Papike et al. 2006). Therefore, terrestrial analog studies for martian jarosite should include samples from a variety of environments. Navrotsky et al. (2005) and Papike et al. (2006) describe the important information we could acquire from martian jarosite if we can obtain a sample. However, sample return from Mars is a long way into the future. In the meantime, we will search for jarosite in martian meteorites. To be ready for such a discovery, we must better understand the chemistry of jarosite–alunite as a recorder of the aqueous solutions from which it formed.

A particularly good example of alunite–jarosite as a recorder of aqueous fluid evolution is provided by samples from the Goldfield Au-Ag mining district, Nevada (Keith et al. 1979; Papike et al. 2006). Our main focus in this paper is on a sample containing jarosite and alunite (Keith et al. 1979), labeled 185-78-1. This sample is from the Preble Mountain area and occurs in the same locale as the precious metal deposits, but it is not directly associated with the ore deposits. A map showing sample localities is provided in Keith et al. (1979). The other samples examined in this study are also from the Goldfield area and are labeled 90-6, 89-8, and 85-2. These samples contain only alunite and their localities are discussed in detail by Vikre et al. (2005). Geochemical examination of samples 90-6, 89-8, and 85-2 shows alunite-pyrite S-isotope equilibrium temperatures of 215–305 °C for ledge wall rocks, and $^{40}Ar/^{39}Ar$ ages of mineralized ledge alunites of 20.3 to 19.8 Ma (Vikre et al. 2005). The Keith et al. (1979) analysis of alunite and jarosite in sample 185-78-1 shows a jarosite K-Ar age of 20 Ma that is concordant with the age of mineralization. The normal sequence of crystallization in 185-78-1 is alunite followed by jarosite. Initially, alunite formed comb-like growths surrounding silicified rock breccia fragments that extend into fractures and vugs. Then both alunite and jarosite formed crystalline aggregates lining the vugs. In the final stage, jarosite alone crystallized and encrusted the remaining vein walls. Where the aggregates were absent, jarosite filled open spaces among alunite crystals and formed terminations on some. Keith et al. (1979) propose that the two minerals formed in one of two ways: (1) All of the Preble Mountain localities were first deficient in Fe and then were flooded with Fe-rich solutions, or (2) the late-stage hydrothermal fluids underwent changes in Eh and pH, leading to oxidation of Fe^{2+} in solution to Fe^{3+} and precipitation of jarosite. In this paper, we report new data for major and minor elements in Goldfield alunite and jarosite to distinguish between the two Keith et al. (1979) models, and

* E-mail: jkarner@unm.edu

0003-004X/06/0007–1197$05.00/DOI: 10.2138/am.2006.2257

also gain additional insights into how chemical zoning in alunite–jarosite records fluid evolution.

Analytical techniques

All analyses reported in this paper were performed on a JEOL 8200 electron microprobe (EMP) at the Department of Earth and Planetary Sciences/Institute of Meteoritics, University of New Mexico. The EMP is equipped with five wavelength dispersive (WD) X-ray spectrometers and an ultrathin-window energy dispersive spectrometer (EDS). Heating under the electron beam and resulting volatilization of water, Na, K, and S are a concern during analysis of jarosite and alunite. Optimum analytical conditions were determined by tuning the WD spectrometer to the Na peak and testing various conditions while watching for any decrease in count rate. We normalized the data collected here to 14 oxygen atoms or 28 negative charges, which is equivalent to formula anions of 8 oxygen atoms and 6 (OH) groups. We cannot analyze for H with the electron microprobe, but the stoichiometry we determine for these samples argues for 6 (OH) groups; we did not detect chlorine in the samples. Given the chemical complexity of these minerals (Scott 1987; Papike et al. 2006), in future studies we may have to use a different normalization scheme. The quality of the analyses was double checked by comparing crystallographic site totals; high B-site and low A-site cation totals (see discussion below) are an indication of volatilization. Optimum conditions for WD analysis of major and minor elements were determined to be 10 nA beam current and a 10 μm spot size at 15 kV. Counting times were 20 s for major elements and 40 s for minor elements. The large spot size, however, tended to average out any small scale zoning present in the jarosite, so a second set of conditions was used for EDS analyses of major elements only, to reveal fine scale zoning. In this case, spectra were collected for 30 s using a 1 nA and 1 μm spot size at 15kV. However, even a 1 μm beam cannot resolve the narrow bands and thus, averages over several bands.

Results and discussion

Although more than 40 mineral species have the fundamental alunite crystal structure (Stoffregen et al. 2000), this paper concerns only alunite, $KAl_3(SO_4)_2(OH)_6$; natroalunite, $NaAl_3(SO_4)_2(OH)_6$; jarosite, $KFe^{3+}_3(SO_4)_2(OH)_6$; and natrojarosite, $NaFe^{3+}_3(SO_4)_2(OH)_6$. We use the general formula $AB_3(XO_4)_2(OH)_6$ (Scott 1987) where A is a 12-fold coordinated site that can contain monovalent cations K, Na, Rb, etc., divalent cations Ca, Pb, Ba, Sr, etc., and trivalent cations, REE, etc. The B position represents an octahedral site that usually contains trivalent Fe and Al but can also include Zn^{2+}, Mg^{2+}, etc. The X position represents the tetrahedral site and contains S, P, As, Sb, etc. For more discussion of alunite-jarosite crystal chemistry, refer to Papike et al. (2006).

Table 1. Representative analyses for Goldfield, Nevada alunite and jarosite

Probe point	1-9	2-10	2-5	2-6	2-9
Description	Alunite	Alunite	Jarosite	light jarosite	dark jarosite
Al_2O_3	37.7	37.8	0.46	0.16	0.48
SO_3	37.9	38.1	32.1	32.2	33.0
Na_2O	0.72	0.45	1.96	0.56	3.68
Fe_2O_3	0.07	0.33	46.8	47.1	47.1
K_2O	10.3	9.95	7.19	8.70	4.66
P_2O_5	0.14	0.13	0.11	0.06	0.03
As_2O_5	0.00	0.00	0.30	0.24	0.00
CaO	0.00	0.00	0.07	0.00	0.00
MoO_3	0.00	0.00	0.04	0.04	0.00
(H_2O)*	13.1	13.2	10.9	10.9	11.0
(Total)†	100	100	100	100	100
Cations based on 14 oxygen atoms					
Al	3.06	3.05	0.04	0.02	0.05
Fe^{3+}	0.00	0.02	2.91	2.94	2.89
Sum B-site	3.06	3.07	2.95	2.96	2.94
S	1.96	1.96	1.99	2.01	2.02
P	0.01	0.01	0.01	0.00	0.00
As	0.00	0.00	0.01	0.01	0.00
Sum T-site	1.97	1.97	2.01	2.02	2.02
Na	0.10	0.06	0.31	0.09	0.58
K	0.91	0.87	0.76	0.92	0.48
Ca	0.00	0.00	0.01	0.00	0.00
Sum A-site	1.01	0.93	1.08	1.01	1.06
Calculated H	6.0	6.1	6.0	6.0	6.0
Total Cations	12.0	12.1	12.0	12.0	12.0

Notes: The probe point label refers to a location in either Figure 1 or 2 and the corresponding analysis number.
* Calcuated by difference.
† Assume 100% sum.

We started our analytical work by doing complete WDS scans on each sample to determine which elements were detectible by EMP. All analyses fell close to the alunite–jarosite quadrilateral compositions (QUAD) defined by the end-members alunite-jarosite-natroalunite-natrojarosite. The data are displayed in Figures 1–4 and representative analyses are included in Table 1. Papike et al. (2006) also present back-scattered electron (BSE) images and X-ray maps for the alunite–jarosite assemblages. Figures 1 and 2 show BSE images of alunite (A) and jarosite (J), and selected WDS EMP analyses keyed to each image. Within each mineral phase, there are various degrees of contrast where darker areas reflect higher Na. Sharp contacts between alunite and jarosite, and jarosite overgrowth on alunite are clearly seen in the lower part of Figure 1. Figure 2 shows spectacular relationships between alunite and jarosite, again showing the

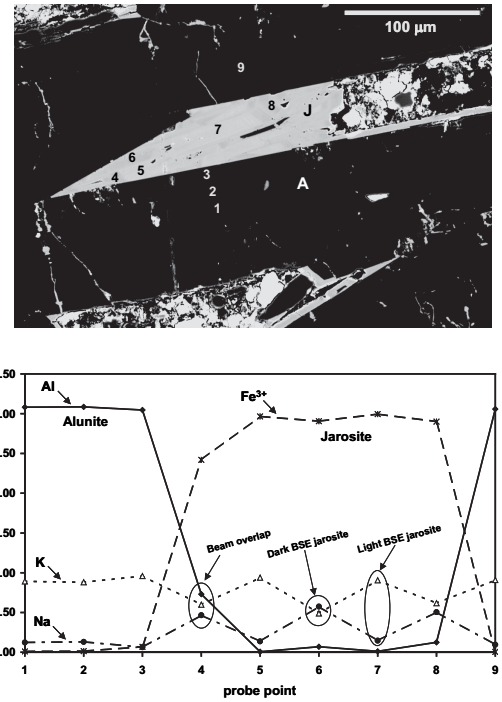

Figure 1. BSE image of alunite (A) and jarosite (J) and corresponding WDS EMP analyses with a 10 μm beam. The plot shows jarosite and alunite compositions with respect to Fe^{3+}, Al, K, and Na reported in atoms per formula unit (afu). Representative complete analyses from this figure are reported in Table 1 where, for example, probe point 1-9 refers to Figure 1, point 9. Note the overgrowth of jarosite (light) over alunite (dark) in the lower central part of the BSE image.

overgrowth of jarosite on alunite. If there was a significant temporal interruption between the alunite and jarosite forming solutions, it did not result in any erosion of the alunite growth surfaces. Note also the patchy color contrast in alunite and the oscillatory banding in jarosite. The 10 μm beam used in these WDS analyses did not resolve the fine compositional variations between the bands, but averaged the chemical contrast between several thin bands. Figure 3 is a false-color BSE image of the center part of Figure 2, and also indicates a corresponding EDS traverse with a 1 μm beam diameter, which better resolves the Na-K banding in jarosite, but not completely.

Figure 4 shows the EMP data on the QUAD plot. Jarosite from Peña Blanca, Mexico (see Lueth et al. 2005) is also plotted for comparison. The diagram shows a significant range in Na/K in both alunite (4 samples) and jarosite (1 sample). Peña Blanca jarosite has no detectable Na. These data indicate significant differences between the fluids that formed the Peña Blanca jarosite and those forming the Goldfield alunite–jarosite. The Goldfield fluids were considerably richer in Na. Note also on the QUAD plot that jarosite can have a significant Al content, but alunite has little Fe^{3+}. This is important because there is no crystal chemical reason for a large miscibility gap between alunite and jarosite. Aluminum and Fe^{3+} are similar in size, identical in charge, and thus freely substitute for each other in the B octahedral sites in the crystal structure (see Papike et al. 2005, Fig. 2). Our interpretation of these chemical systematics is that f_{O_2} is the important controlling factor and is basically responsible for an "on-off switch" behavior between the two phases. In the alunite stability field, the Fe in solution is Fe^{2+}, which is incompatible in the alunite crystal structure. Ferrous iron is incompatible in the alunite crystal structure because it is significantly larger than the Al it substitutes for and also has a different charge, and thus requires a coupled substitution. See Papike et al. (2006) for a more complete discussion. However, in the jarosite stability field, fluids containing high Al in solution will result in Al substitution for Fe^{3+} in the jarosite B-sites.

Papike et al. (2006, Fig. 13) present an Eh-pH diagram simplified from Keith et al. (1979) showing a fluid evolution trajectory from higher pH, lower Eh fluids, to lower pH, higher Eh solutions. We prefer this model (model 2 of Keith et al. 1979) and believe the abrupt transition from alunite to jarosite crystallization was triggered by an oxidant (perhaps oxygen) entering the system, which oxidized Fe^{2+} to Fe^{3+}, raised the Eh, and perhaps lowered the pH by oxidizing any H_2S in the fluids (Papike et al. 2006).

Deyell and Dipple (2005) studied the effects of temperature and bulk fluid K/Na on the alunite-natroalunite solid solution at 200 bars and 100–300 °C. Their model is based on published experimental parameters that indicate that both alunite and natroalunite are stable over this temperature range and increased

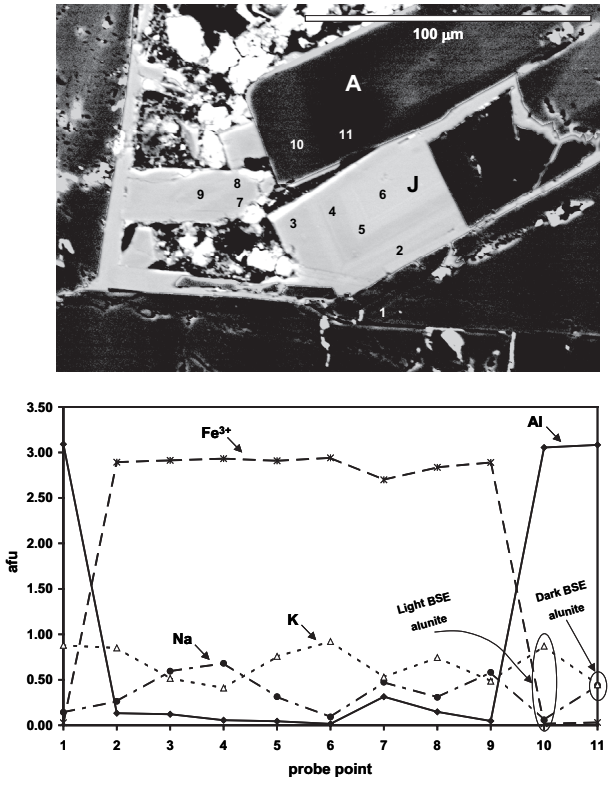

FIGURE 2. BSE image of alunite (A) and jarosite (J) and corresponding WDS EMP analyses (10 μm beam) reported in the bottom plot as Fe^{3+}, Al, K, and Na afu in either jarosite or alunite. Complete analyses for points 2-5, 2-6, 2-9, and 2-10 are shown in Table 1.

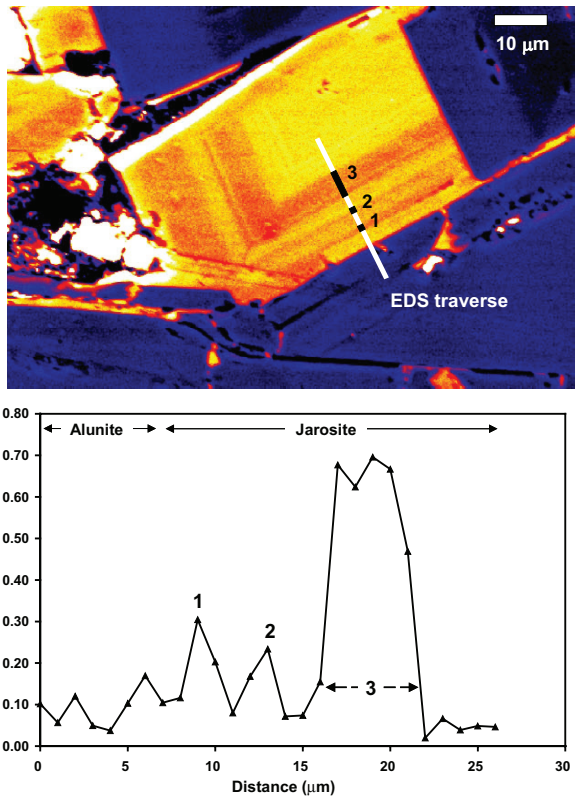

FIGURE 3. False-color BSE image magnifying the central area of Figure 2, and corresponding plot of EDS EMP traverse with a 1 μm beam. The plot shows the traverse with respect to Na/Na + K (atomic) and highlights the locations of points 1, 2, and band 3 on the image.

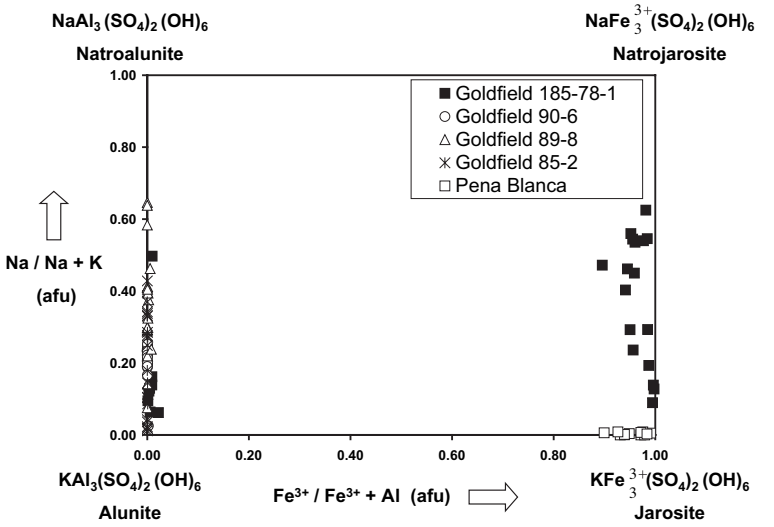

FIGURE 4. Alunite-jarosite QUAD plot. Goldfield 185-78-1 is from Keith et al. 1979; Goldfield 90-6, 89-8, and 85-2 are from Vikre et al. 2005. The Peña Blanca sample is described in Lueth et al. 2005. All plotted data were collected in this study.

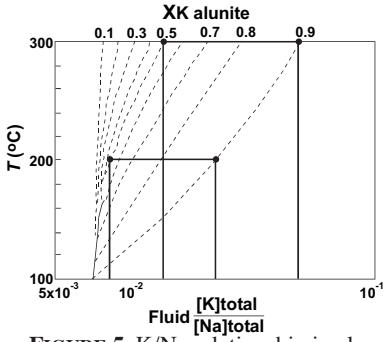

FIGURE 5. K/Na relationship in alunite and coexisting fluid with respect to temperature. Alunite X_K is equal to K/K + Na (atomic). See text for discussion.

Na substitution is favored at higher temperatures. The modeling results indicate that a large variation in fluid K/Na is required to precipitate both K- and Na-alunite at high temperatures. At lower temperatures, much less variation in fluid composition can yield compositions near those of the end-members.

Figure 5 illustrates the Deyell and Dipple (2005) model. On the diagram, bulk fluid K/Na is plotted vs. temperature for compositions of mol% K (K/K+Na -atomic) in alunite from 0.1 to 0.9. The solid line represents the position of the solvus between Na-alunite solid solutions and K-alunite solid solutions. The diagram shows that significant changes in equilibrium-fluid K/Na occur with increasing temperature at each solid solution composition. This research indicates that estimates of the fluid K/Na ratio can be made if the K/Na ratio of the alunite can be determined and an independent estimate of the temperature of deposition can be made.

On Figure 5, we plot the fluid K/Na ratios for temperatures of 200 and 300 °C. The solid solution range between alunite and natroalunite approximates what we observe (Fig. 4). The implications of this plot are that the crystals (especially jarosite) grew quickly, and delivery of free Na or K to the crystal growth surface could not keep up with crystal growth, resulting in oscillatory zoning in jarosite and even the patchy zoning in alunite. The large fluctuations in the jarosite (if the alunite diagram is applicable) K/Na ratio indicate up to an order of magnitude variation of K/Na ratio of the fluid at the crystal-fluid interface. This may be a result of Na and K diffusion rates in the fluid, but also may be a result of any complex ions of Na and K in solution. Then, the rate controlling step for delivery of Na or K to the growth surface is determined by the kinetics of complex ion breakdown.

ACKNOWLEDGMENTS

A NASA Cosmochemistry Grant to JJP, which we gratefully acknowledge, supported this research. We also thank Heather A. Lowers and an anonymous reviewer for their constructive comments. We thank Roger Ashley and Peter Vikre for providing samples and important scientific input as to their geological significance.

REFERENCES CITED

Deyell, C.L. and Dipple, G.M. (2005) Equilibrium mineral-fluid calculations and their application to the solid solution between alunite and natroalunite in the El Indio-Pascua belt of Chile and Argentina. Chemical Geology, 215, 219–234.

Keith, W.J., Calk, L., and Ashley, R.P. (1979) Crystals of coexisting alunite and jarosite, Goldfield, Nevada. Shorter contributions to mineralogy and petrology, U.S. Geological Survey Professional Paper 1124-C, C1–C5.

Klingelhöfer, G., Morris, R.V., Bernhardt, B., Shröder, C., Rodinov, D.S., de Souza, P.A., Yen, A., Gellert, R., Evlanov, E.N., Zubkov, B., Foh, J., Bonnes, U., Kankeleit, E., Gütlich, P., Ming, D.W., Renz, F., Wdowiak, T., Squyres, S.W., and Arvidson, R.E. (2004) Jarosite and hematite at Meridiani Planum from Opportunity's Mössbauer spectrometer. Science, 306, 1740–1745.

Lueth, V.W., Rye, R.O., and Peters, L. (2005) "Sour gas" hydrothermal jarosite: ancient to modern acid-sulfate mineralization in the southern Rio Grande Rift. Chemical Geology, 215, 339–360.

McCollom, T.M. and Hynek, B.M. (2005) A volcanic environment for bedrock diagenesis at Meridiani Planum on Mars. Nature, 438, 1129–1131.

McLennan, S. M., Bell, J.F., III, Calvin, W.M., Christensen, P.R., Clark, B.C., de Souza, P.A., Farrand, W.H., Fike, D., Gellert, R., Ghosh, A., Glotch, T.D., Grotzinger, J.P., Hahn, B., Herkenhoff, K.E., Hurowitz, J.A., Johnson, J.R., Johnson, S.S., Jolliff, B., Klingelhöfer, G., Knoll, A.H., Learner, Z., Malin, M.C., McSween, H.Y., Jr., Pocock, J., Ruff, S.W., Squyres, S.W., Tosca, N.J., Watters, W. Wyatt, M.B., Yen, A., and the Athena Science Team (2005) Provenance and diagenesis of impure evaporitic sedimentary rocks on Meridiani Planum, Mars. Lunar and Planetary Science XXXVI, no. 1884, Lunar and Planetary Institute, Houston, Texas, CD-ROM.

Navrotsky, A., Forray, F.L., and Drouet, C. (2005) Jarosite stability on Mars. Icarus, 176, 250–253.

Papike, J.J., Karner, J.M., and Shearer, C.K. (2005) Comparative planetary mineralogy: Valence state partitioning of Cr, Fe, Ti, and V among crystallographic sites in olivine, pyroxene, and spinel from planetary basalts. American Mineralogist, 90, 277–290.

——— (2006) Comparative planetary mineralogy: Implications of martian and terrestrial jarosite. A crystal chemical perspective. Geochimica et Cosmochimica Acta, 70, 1309–1321.

Scott, K.M. (1987) Solid solution in, and classification of, gossan-derived members of the alunite-jarosite family, northwest Queensland, Australia. American Mineralogist, 72, 178–187.

Stoffregen, R.E., Alpers, C.N., and Jambor, J.L. (2000) Alunite-jarosite crystallography, thermodynamics, and geochronology. In C.N. Alpers, J.L. Jambor, and D.K. Nordstrom, Eds., Sulfate Minerals—Crystallography, Geochemistry, and Environmental Significance, 40, p. 453–479. Reviews in Mineralogy and Geochemistry, Mineralogical Society of America, Chantilly, Virginia.

Vikre, P., Fleck, R., and Rye, R. (2005) Ages and geochemistry of magmatic hydrothermal alunites in the Goldfield district, Esmeralda Co., Nevada. U.S. Geological Survey Open-File Report 2005-1258.

MANUSCRIPT RECEIVED MARCH 6, 2006
MANUSCRIPT ACCEPTED MARCH 27, 2006
MANUSCRIPT HANDLED BY BRYAN CHAKOUMAKOS